Revisiting the parameterization of potential evaporation as a driver of long-term water balance trends

Michael T. Hobbins,[1] Aiguo Dai,[2] Michael L. Roderick,[1] and Graham D. Farquhar[1]

Received 4 March 2008; revised 10 April 2008; accepted 16 April 2008; published 20 June 2008.

[1] We examine the effects of two different parameterizations of potential evaporation on long-term trends in soil moisture, evaporative flux and runoff simulated by the water balance model underlying the Palmer Drought Severity Index. The first, traditional parameterization is based on air temperature alone. The second parameterization is derived from observations of evaporation from class-A pans. Trends in potential evaporation from the two parameterizations are opposite in sign (±) at almost half the stations tested over Australia and New Zealand. The sign of trends in the modelled soil moisture, evaporative flux and runoff depends on the parameterization used and on the prevailing climatic regime: trends in water-limited regions are driven by precipitation trends, but the choice of parameterization for potential evaporation is shown to be critical in energy-limited regions. **Citation:** Hobbins, M. T., A. Dai, M. L. Roderick, and G. D. Farquhar (2008), Revisiting the parameterization of potential evaporation as a driver of long-term water balance trends, *Geophys. Res. Lett.*, *35*, L12403, doi:10.1029/2008GL033840.

1. Introduction

1.1. Background

[2] Simple water balance models are often used to assess land surface moisture conditions. A typical example is the water balance model underlying calculations of the Palmer Drought Severity Index (PDSI) [*Palmer*, 1965]. Routinely used in the US to assess developing drought conditions, this model was recently extended on a worldwide, long-term basis leading to the conclusion that many regions have become drier and more drought-affected during recent decades [*Dai et al.*, 2004]. In the PDSI, the water-balance is calculated using a bucket model, yielding a moisture anomaly from which the non-dimensional, monthly drought index is derived. In the bucket model, soil fills with precipitation (*Prcp*) and empties through actual evapotranspiration (ET_a) and *Runoff*. At each model time step, the maximum possible ET_a is the minimum of the evaporative demand, herein denoted potential evaporation (E_p), and the available water.

1.2. Water- and Energy-Limited Environments

[3] E_p and ET_a can be considered in the classical framework of the limitations on ET_a. In environments with a limited supply of soil-water to evaporate, ET_a is less than E_p. In these "water-limited" environments, it is changes in the availability of water (through *Prcp*), and not of energy, that dominate changes in ET_a. As water availability increases, ET_a converges towards E_p until they are equal in wet environments. Here only the availability of energy limits ET_a, and in such "energy-limited" environments, increasing *Prcp* will not change ET_a but will increase soil moisture and/or *Runoff*. Increasing the availability of energy alone at energy-limited sites will raise ET_a and consequently depress soil moisture and/or *Runoff*. Most regions in the world lie in the continuum between the water and energy limits, reaching either only seasonally. The method used to estimate E_p (and hence constrain ET_a) influences the water balance calculation and the resulting conclusions on long-term trends, hence it is the effects of different E_p formulations on long-term water balance variables that motivate this paper.

1.3. E_p Trends

[4] In the traditional formulation of the PDSI bucket model, evaporative demand is derived from an approach that can be traced back to *Thornthwaite* [1948] and is solely a function of air temperature (T_{air}). Consequently, as T_{air} steadily increases with global warming, the calculated value of E_p in the model also steadily increases. In contrast, the measurements of pan evaporation (E_{pan}) that are better physical representations of E_p show widespread declines over the last 30-50 years [*Peterson et al.*, 1995; *Chattopadhyay and Hulme*, 1997; *Golubev et al.*, 2001; *Hobbins et al.*, 2004; *Liu et al.*, 2004; *Roderick and Farquhar*, 2004, 2005; *Tebakari et al.*, 2005; *Wu et al.*, 2006]. Similarly, calculations of reference *ET* [*Allen et al.*, 1998] (also see auxiliary material[1]) using observations of solar radiation, T_{air}, humidity, and wind speed also show declines [*Thomas*, 2000; *Chen et al.*, 2005; *Shenbin et al.*, 2006], in general agreement with the E_{pan} record in China. The poor performance of T_{air}-based E_p in predicting observed evaporative demand was further highlighted in China, where rising T_{air} but declining E_{pan} were found across eight of the 10 river basins [*Chen et al.*, 2005].

[5] The key point here is that E_p is less affected by changes in T_{air} than by changes in surface radiation, wind speed, and humidity deficit [*Roderick et al.*, 2007]. Indeed, when formulating the PDSI, *Palmer* [1965] recognized the importance of all of these dynamics driving the more physically complete *Penman* [1948] E_p-formulation, but justified his choice of an equation for E_p based solely on T_{air} by an appeal to expediency, having previously noted, "...Thornthwaite's empirical formula can be used for any location at which daily maximum and minimum temperatures are recorded. It is this simple universal applicability

[1]Environmental Biology Group, Research School of Biological Sciences, Australian National University, Canberra, A.C.T., Australia.
[2]National Center for Atmospheric Research, Boulder, Colorado, USA.

0094-8276/08/2008GL033840$05.00

[1]Auxiliary materials are available in the HTML. doi:10.1029/2008GL033840.

Table 1. Magnitude, Range, Direction, and Significance of Temporal Trends for the Inputs and Both Parameterizations' Outputs Across the Two Sets of Stations[a]

Parameterization	Variable	Trend Statistics			Trend Direction (# $p \leq 0.05$)	
		Mean ± Stdev	Min	Max	+ve	−ve
		Australia, 27 stations, 1975–2004				
Observed	*Prcp*	0.10 ± 3.92	−10.31	6.84	14 (1)	13 (1)
	T_{air}	0.01 ± 0.01	−0.01	0.03	22 (6)	5 (0)
	E_{pan}	−2.67 ± 7.62	−17.48	10.95	10 (3)	17 (7)
E_p^{PDSI}	E_p	1.14 ± 1.25	−0.59	3.83	20 (6)	7 (0)
	ET_a	0.45 ± 3.02	−9.37	6.71	16 (2)	11 (1)
	SM	−0.27 ± 0.99	−3.75	0.99	13 (0)	14 (2)
	Runoff	−0.50 ± 1.72	−7.52	1.25	17 (0)	10 (0)
E_p^{Pan}	E_p	−2.00 ± 5.72	−13.11	8.22	10 (3)	17 (7)
	ET_a	0.15 ± 3.20	−9.66	6.76	14 (1)	13 (1)
	SM	−0.05 ± 0.94	−3.94	1.17	14 (0)	13 (2)
	Runoff	−0.14 ± 2.02	−6.68	6.24	18 (0)	9 (1)
		New Zealand, 8 stations, 1974–2003				
Observed	*Prcp*	−3.24 ± 6.34	−12.16	4.88	3 (0)	5 (4)
	T_{air}	0.02 ± 0.01	−0.01	0.04	7 (3)	1 (0)
	E_{pan}	−1.77 ± 2.21	−4.74	0.89	3 (0)	5 (2)
E_p^{PDSI}	E_p	1.03 ± 0.98	−0.49	2.54	7 (3)	1 (0)
	ET_a	0.51 ± 1.55	−2.14	2.51	6 (2)	2 (0)
	SM	0.19 ± 0.64	−1.55	0.39	5 (1)	3 (1)
	Runoff	−3.58 ± 5.80	−12.90	4.75	3 (0)	5 (4)
E_p^{Pan}	E_p	−1.24 ± 1.55	−3.32	0.62	3 (0)	5 (2)
	ET_a	−0.89 ± 2.77	−5.58	2.36	4 (1)	4 (2)
	SM	−0.05 ± 0.61	−0.94	0.88	5 (1)	3 (2)
	Runoff	−2.21 ± 4.83	−8.83	4.83	3 (0)	5 (3)

[a]Units are mm/year^2 for trends in *Prcp*, E_{pan}, E_p, ET_a, and *Runoff*; °C/year for trends in T_{air}; and mm/year for trends in *SM*. Means and standard deviations are across the 27 stations in Australia and eight stations in New Zealand. Numbers in parentheses count trends significant at 95%.

rather than any claim to outstanding accuracy which has led to the widespread use of this method'' [*Palmer and Havens*, 1958]. In fact, *Thornthwaite* [1948], too, expected his T_{air}-based approach to be replaced by a more physically based method as the necessary theory was developed and supporting data became more widely available. As evaporation from a water surface inside a pan integrates all these factors [*Rotstayn et al.*, 2006], its measurements have long been widely used as a physical measure of E_p in agricultural and engineering applications. While other workers have examined the sensitivity of long-term PDSI to various model features [e.g., *Karl*, 1986], no-one has yet examined the effects of using such a physically based E_p.

[6] Clearly, the declining trend in physically based measures of E_p compared to the increasing trend implied by calculations based solely on T_{air} might lead to different conclusions about trends in drying [*Moonen et al.*, 2002]. In this paper, we examine that proposition by running the PDSI water balance model at 35 sites across Australia and New Zealand. At each site, the model is run twice. In the first run, we calculate E_p per the standard PDSI implementation using T_{air} measurements. In the second run, E_p is based on pan evaporation observations. No other forcings (e.g., *Prcp*) and model parameters are changed, thereby isolating the effect of different formulations of evaporative demand on the outputs of the water balance model (ET_a, soil moisture, and *Runoff*) and hence on the modelling of drought.

2. Methods and Materials

2.1. Description of the Water Balance Model

[7] The PDSI bucket model uses a two-layer soil column, with the water content at field capacity set as 25.4 mm (1 inch) for the upper layer, where it is assumed freely available for evapotranspiration, and that for the lower layer (or root zone) prescribed by the analyst. Evaporative demand in the PDSI is traditionally set as a time-series of T_{air}-based E_p. *Prcp* is partitioned into recharge, filling first the upper soil layer and then the lower layer, until the soil column fills; *Runoff* occurs when whole-column soil moisture (*SM)* is at field capacity and evaporative demand (i.e., E_p) from both layers has been met. When *Prcp* and upper-layer soil moisture cannot meet E_p, the soil dries in two stages: moisture in the upper soil-layer completely evaporates at the potential rate (i.e., E_p), then that in the root-zone declines at a rate depending on root-zone soil moisture and unmet E_p. Note that the physiologic response of vegetation to water limitation is modelled in this two-layer soil column, not in the parameterization of evaporative demand. The water-equivalent depth of the bucket (*AWC*) was set using the same 2.5° × 2.5° global grid used by *Dai et al.* [2004] (see Figure S1a).

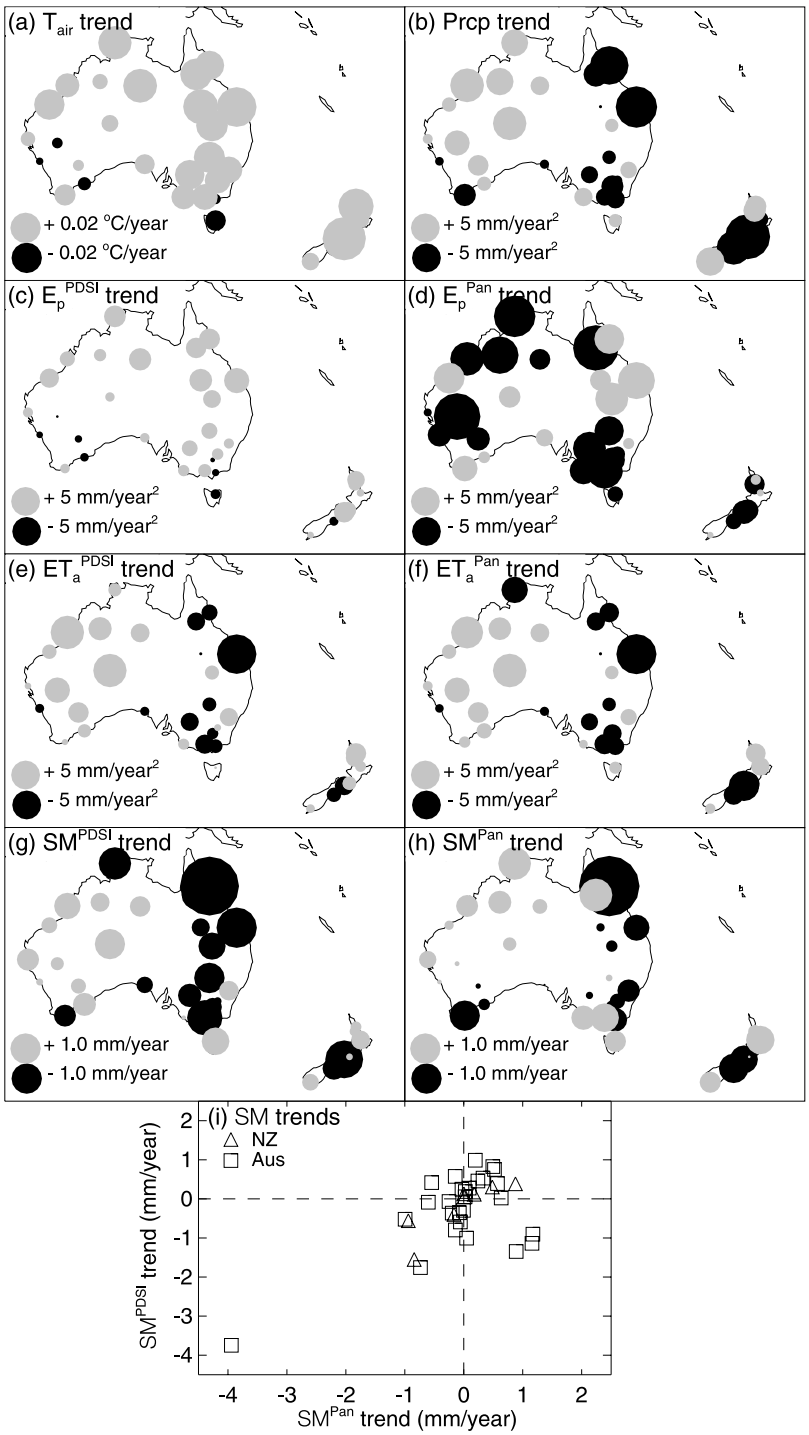

Figure 1. Annual trends at 27 stations in Australia and eight in New Zealand over the periods 1975–2004 (Australia) and 1974–2002 (New Zealand). Maps show direction and scale of trends for (a) T_{air}, (b) $Prcp$, (c) E_p^{PDSI}, (d) E_p^{Pan}, (e) ET_a^{PDSI}, (f) ET_a^{Pan}, (g) SM^{PDSI}, and (h) SM^{Pan}. Grey circles indicate positive trends, black circles negative, with areas proportional to trend magnitudes. In (i) the station-trends in SM^{PDSI} (Figure 1g) are plotted against those in SM^{Pan} (Figure 1h).

2.2. Data and Study Area

[8] We chose Australia and New Zealand as our study area. This represents a wide climatologic range because Australia is primarily water-limited and New Zealand energy-limited (see section SI.3 and Figure S3). Australian stations were restricted to the 27 sites with monthly T_{air}, $Prcp$, and E_{pan} data used by *Roderick et al.* [2007] that were also part of the High Quality Annual T_{air} data network [*Della-Marta et al.*, 2004]. The period of analysis for Australian data was 1975-2004. We selected the eight New Zealand sites for which long-term monthly $Prcp$, T_{air}, and E_{pan} records were available from the National Institute of Water and Atmospheric Research (NIWA). Analysis periods varied across the New Zealand sites but were constrained to within 1974–2003 (see Table S2).

[9] As the soil moisture-accounting in the PDSI bucket model requires continuous monthly input time-series, missing data were filled as follows: (i) when only one or two months' data were missing from a year, these monthly data were scaled from their climatological monthly means according to the proportion in the rest of the year; or (ii) when over two months' data were missing from a given year, all months of that year were replaced by their climatological means. In the worst case (E_{pan} for New Zealand), less than 3% of data were infilled. For further details on data sources, see section SI.2.

2.3. Two Estimates of E_p

[10] Our first estimate of E_p is that used operationally in the PDSI by NOAA [*Dai et al.*, 2004], and here denoted E_p^{PDSI} (see equations (S1)-(S3)). The constant heat factors (B and H, see equation (S2)) required for E_p^{PDSI} were prescribed using the 2.5° × 2.5° global grids from *Dai et al.* [2004] (see Figures S1b and S1c). Our second E_p estimate uses observed monthly E_{pan} multiplied by the traditional pan coefficient k, i.e., $E_p^{Pan} = k.E_{pan}$. While k has been shown to vary seasonally [*Allen et al.*, 1998], the widely adopted value of 0.7 [*Stanhill*, 1976] was used for the unscreened New Zealand pans. For the Australian pans, k was set to 0.75 to account for the 7% reduction in E_{pan} due to the bird-guards [*van Dijk*, 1985].

2.4. Model Calculations

[11] In running the PDSI bucket model, initial *SM* was specified equal to *AWC*, for the following reasons: first, it is standard PDSI procedure to initiate the model run with maximum moisture in both soil layers; second, a sensitivity analysis (not shown) indicated that the effects of initial conditions disappeared within two years. Nonetheless, to eliminate bias and minimize the effects of high initial *SM* conditions, the models were run for two years prior to the analysis period. Trends were defined as the slope of an Ordinary Least Squares regression through annual time-series, with the significance of annual trends determined by *t*-tests. As the model conserves mass, the trends in the component fluxes (*Prcp*, ET_a, and *Runoff*) sum to the second time-differential of *SM*. We report the first time-differential of *SM* as it is of greatest climatological interest.

3. Results

[12] The observed trends in the input time-series—T_{air} (for the E_p^{PDSI} run), *Prcp* (for both runs), and $k.E_{pan}$ (for the E_p^{Pan} run)—are shown in Figures 1a, 1b, and 1d, respectively, and closely match previous results for Australia and New Zealand [*Roderick and Farquhar*, 2004, 2005]. The difference between the two E_p measures is apparent in Figures 1c and 1d. Note that of the 35 sites, most (27) show increases in E_p^{PDSI}, in line with the general increase in T_{air} shown in Figure 1a. In contrast, only 13 sites showed increases in E_p^{Pan}.

[13] ET_a-trends in Australia (Figures 1e and 1f) generally follow the *Prcp*-trends (Figure 1b). This result is expected because Australia is largely water-limited (section SI.3 and Figure S3), so trends in moisture supply, not in evaporative demand, largely determine the ET_a-trend. However, in New Zealand, whether ET_a-trends increased or decreased depended on the E_p parameterization. Again, this result is expected because at energy-limited sites, ET_a is sensitive to changes in E_p. Clearly, ET_a^{Pan} in New Zealand responds to dynamics in evaporative demand missing from the E_p^{PDSI} parameterization. While differences exist between the scale and direction of *SM*-trends, both parameterizations generate generally declining *SM* in eastern Australia and central New Zealand, with increases in western Australia and northern and southern New Zealand (Figures 1g and 1h). Again, in Australia, both models generate spatial patterns of *SM*-trends more closely resembling trends in *Prcp* than in E_p. Figure 1i shows the relations between *SM*-trends between the two parameterizations at all stations mapped in Figures 1g and 1h. Clearly, there is little relationship between the *SM*-trends predicted using E_p^{PDSI} and E_p^{Pan}: at seven of the 35 stations, they are of different signs, and five of these stations are located in important agricultural and/or populated regions of southwestern Western Australia, New South Wales, and Victoria.

[14] The potential for mismatch between the hydrologic trends estimated by the two parameterizations is further demonstrated at Darwin (the northernmost station in the Australian set), which is energy-limited on an annual basis. Here moisture supply is increasing ($dPrcp/dt$ = +4.4 mm/year^2), but the E_p-parameterizations' respective drivers are in conflict: warming leads to increasing E_p^{PDSI} (dT_{air}/dt = +0.02°C/year, dE_p^{PDSI}/dt = +2.8 mm/year^2), but E_{pan} is decreasing (dE_p^{Pan}/dt = -10.4 mm/year^2) due to declining wind speeds and solar radiation [*Rayner*, 2007; *Roderick et al.*, 2007]. The decline in the energy available for evaporation is captured by the E_p^{Pan} observations, but not by the E_p^{PDSI} calculations because the latter do not respond to solar radiation or wind speed. Thus, the two parameterizations drive the PDSI bucket model to indicate opposite trends in ET_a (dET_a^{PDSI}/dt = +1.1 mm/year^2, dET_a^{Pan}/dt = -4.2 mm/year^2), which leads to the soil drying in the case of E_p^{PDSI} (dSM^{PDSI}/dt = -1.1 mm/year) and wetting in the case of E_p^{Pan} (dSM^{Pan}/dt = +1.2 mm/year).

4. Discussion

[15] In assessing the likely ecohydrologic impacts of climate change, projections of continental drying must be reconciled with observations of declining evaporative demand. The PDSI, upon which much support for many of these conflicting projections is based, is an index based on a hydrologic model that predicts evaporative demand from the direct effect of surface warming only. However, the effects of other accompanying changes, such as those in surface radiation, wind speed and humidity, likely play an important role over many land areas [*Roderick et al.*, 2007].

[16] Here we have compared long-term trends in ET_a and *SM* from the PDSI bucket model forced by two parameterizations of E_p: one based on T_{air} alone; the other derived from observations of a physical metric of evaporative demand (i.e., E_{pan}) that responds to the appropriate dynamics—T_{air}, humidity, wind speed, and net available energy [*Rotstayn et al.*, 2006]. The primary attraction of the T_{air}-based E_p^{PDSI} is simplicity: only T_{air} data are required, and such data are widely available in time and space, including historical global grids at many spatio-temporal resolutions. That historical T_{air}-trends are more certain than trends in radiation, humidity, and wind speed, demonstrates the value

of the E_{pan} record: these variables are physically integrated into E_{pan} measurements. Here we have shown that T_{air}-based E_p cannot predict the directions of observed trends in evaporative demand: 46% of the long-term trend directions predicted by E_p^{PDSI} are opposite to those observed in E_{pan} across Australia and New Zealand.

[17] It is important to note that using T_{air}-based parameterizations in climate change analyses—particularly in deriving trends in drought dynamics—invokes retrograde assumptions about the relationships of T_{air} to all other evaporative drivers. In fact, using T_{air}-based E_p produces an apparent paradox with declining E_{pan} in Australia, which has been resolved by *Roderick et al.* [2007] as caused by reductions in wind speed and some regional changes in solar radiation—both drivers unaccounted for in a T_{air}-based E_p. It can be no surprise then that T_{air}-based predictions of drying under warming contradict a gathering wealth of reports of decreasing evaporative demand in the face of global warming.

[18] More subtle interactions between trends in the surface water balance arise in energy-limited regions than in water-limited regions, so the answer to the question "does warming mean drying?" depends critically on accompanying changes in *Prcp* and also on the climate regime in question. Our Budyko-based climatological analysis (see Figure S3) indicates that, over water-limited regions such as most of Australia, trends in ET_a are largely determined by trends in *Prcp*, and not in E_p. However, this conclusion does not assist in the essential regional analyses: it is in the southern and eastern regions of Australia—areas that are wetter (i.e., more energy-limited) than the continental mean and, crucially, where most people live and most agricultural production occurs—that the differences in direction and scale of *SM*-trends between parameterizations are most apparent. Here, the E_p parameterization choice is crucial.

[19] Our conclusions regarding the disjunction between drying predicted by T_{air}-based parameterizations and observations of wetting are also implicit in the results of *Robock et al.* [2005], who, working with a large-scale set of observed soil moisture in the Ukraine from 1958 to 2002, found that decreasing summer *Prcp* under a warming trend had still resulted in increased summer soil moisture.

5. Conclusions

[20] Our comparison of different E_p formulations in the PDSI bucket model has highlighted the problems with the T_{air}-based parameterization of evaporative demand classically used in a well-established water balance model (i.e., E_p^{PDSI}). We find that, in energy-limited regions, what constitutes drying under E_p^{PDSI} frequently shows as wetting under E_p^{Pan}. While the analysis here is limited to Australia and New Zealand, our station selection covers a broad climatic range, so we expect our findings—wetting often projected by a physically based parameterization where drying had previously been projected by one that is T_{air}-based—to apply elsewhere, as over the last few decades declining E_{pan} has been widely observed in the face of globally rising T_{air}.

[21] The PDSI model could be parameterized with potential evapotranspiration, such as that from the Penman-Monteith approach. However, the limited availability of data on humidity, solar radiation, wind speed, and surface resistance currently preclude such an observational study on a global or even continental basis, although work progresses on developing such datasets [*Dai et al.*, 2005]. In the meantime, however, results from a multi-model ensemble-mean (see Figure 10.12 in the IPCC AR4 WG1 report [*Meehl et al.*, 2007]) indicate patterns of projected trends in ET_a broadly similar to those in *Prcp* over much of the global land surface.

[22] Our continent-wide results warn against an over-simplistic treatment of evaporative demand in water balance models and highlight the urgent need for a more rigorous approach to assessing long-term changes in the terrestrial water balance. The effects of this over-simplicity may be obscured in water-limited regions as evapotranspiration there is strictly constrained by water availability. However, more rigorous analyses are particularly wanting over regions where evapotranspiration is limited frequently or consistently by the availability of energy, and where this empirical study shows important dependencies of ET_a and *SM* on E_p. Meeting this need over more than select regions presents the hydroclimatological community with the same challenge originally laid down by *Penman* [1948], *Thornthwaite* [1948], and *Palmer* [1965]: to develop reliable global datasets of radiation, humidity and wind as well as air temperature and precipitation to permit physically sound estimations of water balance trends.

[23] **Acknowledgments.** We acknowledge funding support from a Gary Comer Award. We acknowledge the BoM and NIWA and especially the numerous observers whose work formed the ultimate basis of this study. The National Center for Atmospheric Research is sponsored by the U.S. National Science Foundation. Dai is also partly supported by NCAR's Water Cycle Program.

References

Allen, R. G., L. S. Pereira, D. Raes, M. Smith (1998), Crop evapotranspiration: Guidelines for computing crop water requirements, *FAO Irrig. Drain. Pap.*, 56, Food and Agric. Org., Rome.

Chattopadhyay, N., and M. Hulme (1997), Evaporation and potential evapotranspiration in India under conditions of recent and future climate change, *Agric. For. Meteorol.*, *87*, 55–73.

Chen, D., G. Gao, C.-Y. Xu, J. Guo, and G. Ren (2005), Comparison of the Thornthwaite method and pan data with the standard Penman-Monteith estimates of reference evapotranspiration in China, *Clim. Res.*, *28*, 123–132.

Dai, A., T. Trenberth, and K. E. Qian (2004), A global dataset of Palmer Drought Severity Index for 1870–2002: Relationship with soil moisture and effects of surface warming, *J. Hydrometeorol.*, *5*, 117–130.

Dai, A., T. Qian, K. E. Trenberth (2005), Has the recent global warming caused increased drying over land?, paper presented at 16th *Symposium on Global Change and Climate Variations/Symposium on Living with a Limited Water Supply*, Am. Meteorol. Soc., San Diego, Calif.

Della-Marta, P., D. Collins, and K. Braganza (2004), Updating Australia's high-quality annual temperature dataset, *Aust. Meteorol. Mag.*, *53*, 75–93.

Golubev, V. S., J. H. Lawrimore, P. Y. Groisman, N. A. Speranskaya, S. A. Zhuravin, M. J. Menne, T. C. Peterson, and R. W. Malone (2001), Evaporation changes over the contiguous United States and the former USSR: A reassessment, *Geophys. Res. Lett.*, *28*, 2665–2668.

Hobbins, M. T., J. A. Ramírez, and T. C. Brown (2004), Trends in pan evaporation and actual evapotranspiration across the conterminous US: Paradoxical or complementary?, *Geophys. Res. Lett.*, *31*(13), L13503, doi:10.1029/2004GL019846.

Karl, T. R. (1986), Sensitivity of the Palmer Drought Severity Index and Palmer's Z-Index to their calibration coefficients including potential evapotranspiration, *J. Clim. Appl. Meteorol.*, *25*, 77–86.

Liu, B., M. Xu, M. Henderson, and W. Gong (2004), A spatial analysis of pan evaporation trends in China, 1955–2000, *J. Geophys. Res.*, *109*, D15102, doi:10.1029/2004JD004511.

Meehl, G. A., et al. (2007), Global climate projections, in *Climate Change 2007: The Physical Science Basis. Contribution of Working Group 1 to the Fourth Assessment Report of the Intergovernmental Panel on Climate Change*, edited by S. Solomon et al., pp. 749–845, Cambridge Univ. Press, Cambridge, U. K.

Moonen, A. C., L. Ercoli, M. Mariotti, and A. Masoni (2002), Climate change in Italy indicated by agrometeorological indices over 122 years, *Agric. For. Meteorol.*, *111*, 13–27.

Palmer, W. C. (1965), Meteorological drought, Res. Pap. 45, 58 pp., U. S. Dep. of Comm., Washington, D. C.

Palmer, W. C., and A. V. Havens (1958), A graphical technique for determining evapotranspiration by the Thornthwaite method, *Mon. Weather Rev.*, *86*, 123–128.

Penman, H. L. (1948), Natural evaporation from open water, bare soil and grass, *Proc. R. S. London, Series A*, *193*, 120–146.

Peterson, T. C., V. S. Golubev, and P. Y. Groisman (1995), Evaporation losing its strength, *Nature*, *377*, 687–688.

Rayner, D. P. (2007), Wind run changes: The dominant factor affecting pan evaporation trends in Australia, *J. Clim.*, *20*(14), 3379–3394, doi:10.1175/JCLI4181.1.

Robock, A., M. Mu, K. Vinnikov, I. V. Trofimova, and T. I. Adamenko (2005), Forty-five years of observed soil moisture in the Ukraine: No summer dessication (yet), *Geophys. Res. Lett.*, *32*, L03401, doi:10.1029/2004GL021914.

Roderick, M. L., and G. D. Farquhar (2004), Changes in Australian pan evaporation from 1970 to 2002, *Int. J. Climatol.*, *24*, 1077–1090.

Roderick, M. L., and G. D. Farquhar (2005), Changes in New Zealand pan evaporation since the 1970s, *Int. J. Climatol.*, *25*, 2031–2039.

Roderick, M. L., L. D. Rotstayn, G. D. Farquhar, and M. T. Hobbins (2007), On the attribution of changing pan evaporation, *Geophys. Res. Lett.*, *34*, L17403, doi:10.1029/2007GL031166.

Rotstayn, L. D., M. L. Roderick, and G. D. Farquhar (2006), A simple pan-evaporation model for analysis of climate simulations: Evaluation over Australia, *Geophys. Res. Lett.*, *33*, L17715, doi:10.1029/2006GL027114.

Shenbin, C., L. Yunfeng, and A. Thomas (2006), Climatic change on the Tibetan plateau: Potential evapotranspiration trends from 1961–2000, *Clim. Change*, *76*, 291–319.

Stanhill, G., (1976), The CIMO international evaporimeter comparisons, WMO Publ. 449, 38 pp., World Meteorol. Org., Geneva, Switzerland.

Tebakari, T., J. Yoshitani, and C. Suvanpimol (2005), Time-space trend analysis in pan evaporation over Kingdom of Thailand, *J. Hydrol. Eng.*, *10*, 205–215.

Thomas, A. (2000), Spatial and temporal characteristics of potential evapotranspiration trends over China, *Int. J. Climatol.*, *20*, 381–396.

Thornthwaite, C. W. (1948), An approach toward a rational classification of climate, *Geogr. Rev.*, *38*, 55–94.

van Dijk, M. H. (1985), Reduction in evaporation due to the bird screen used in the Australian class A pan evaporation network, *Aust. Meteorol. Mag.*, *33*, 181–183.

Wu, S., Y. Yin, D. Zheng, and Q. Yang (2006), Moisture conditions and climate trends in China during the period 1971–2000, *Int. J. Climatol.*, *26*, 193–206.

A. Dai, National Center for Atmospheric Research, P.O. 3000, Boulder, CO 80307, USA.

G. D. Farquhar, M. T. Hobbins, and M. L. Roderick, Environmental Biology Group, Research School of Biological Sciences, Australian National University, Canberra, ACT 0200, Australia. (michael.hobbins@anu.edu.au)

Auxiliary material for Paper 2008GL033840

Revisiting the parameterization of potential evaporation as a driver of long-term water balance trends

Michael T. Hobbins
Environmental Biology Group, Research School of Biological Sciences, Australian National University, Canberra, A.C.T., Australia

Aiguo Dai
National Center for Atmospheric Research, Boulder, Colorado, USA

Michael L. Roderick and Graham D. Farquhar
Environmental Biology Group, Research School of Biological Sciences, Australian National University, Canberra, A.C.T., Australia

Hobbins, M. T., A. Dai, M. L. Roderick, and G. D. Farquhar (2008), Revisiting the parameterization of potential evaporation as a driver of long-term water balance trends, Geophys. Res. Lett., 35, L12403, doi:10.1029/2008GL033840.

INTRODUCTION

The auxiliary material consists of a text file, three figures, and two tables. The text file provides various definitions and details on parameterizations, data sources, and data-infilling techniques, and summarizes station climatologies and the closure of the water balance. The three figures are maps of data inputs, graphs of the temperature response of evaporative demand as modeled by the traditional PDSI parameterization, and climatologies of the 35 stations. The two tables provide further details on long-term climatological means and trends of the model inputs and outputs broken down on a station-by-station basis for each country's station-sets.

Text file:

2008gl033840-txts01: The text file contains details on the definitions necessary for a more complete understanding of the concept of potential evaporation (Ep); the formulation of the EpPDSI parameterization; the sources and infilling of data used in both Ep parameterizations; the climatologies of the 27 Australian and eight New Zealand stations in terms of the energy- and water-limits on evapotranspiration; the closure of the water balance trends at each station, and the references.

Figures:

2008gl033840-fs01: Maps showing distribution across Australia of (top) AWC in inches derived from Webb et al. [1993], (middle) heat factor B, and (bottom) heat factor H. The heat factors are from Dai et al. [1998] and are used to estimate EpPDSI in equation (S2).

2008gl033840-fs02: Temperature response of the EpPDSI parameterization at latitudes (top) 10 degrees and (bottom) 50 degrees using values of heat factors B and H (min{B, H} = {1.038, 33.973}, max{B,H} = {4.266, 162.602}) encompassing the range of the Australian and New Zealand station sets for mid-winter (blue lines) and mid-summer (red lines). Ordinates are monthly Ep depths, abscissae are mean monthly Tair.

2008gl033840-fs03: Climatologies of the 27 Australian and eight New Zealand stations within the Budyko framework, as represented by observed Prcp, k.Epan, and modeled ETaPan. Wetness and evaporative indices are derived at each station from their long-term mean annual values. Also indicated are the water- and energy-limits on ETa.

Tables:

1. **2008gl033840-ts01:** Station climatologies and trends over the period 1975-2004 at the 27 Australian stations shown in Figure 1 in the text. Population means are derived from the data in this table. Trends are defined as the Ordinary Least Squares-estimated slope of the annual series with respect to time. The residual of the trends in fluxes (dPrcp/dt - dETa/dt - dRO/dt) equals the second differential of SM with respect to time. Asterisks indicate trends significant at 95%.
Columns 1.1-1.5 refer to station identification and geography.
1.1 Column "BoM id", the Bureau of Meteorology (BoM) station identifier.
1.2 Column "Station name ", the BoM station name.
1.3 Column "Long", degrees, station longitude east of Greenwich.
1.4 Column "Lat", degrees, station latitude north of the equator.
1.5 Column "Elev", metres, station elevation above mean sea level.
Columns 1.6-1.11 refer to climatological means and secular trends in observations of model inputs.
1.6 Column "Prcp", mm/year, mean annual precipitation.
1.7 Column "Tair", degrees C, mean annual air temperature.
1.8 Column "Epan", mm/year, mean annual pan evaporation.
1.9 Column "dPrcp/dt", mm/year/year, trend in annual precipitation.
1.10 Column "dTair/dt", degrees C/decade, trend in annual air temperature.
1.11 Column "dEpan/dt", mm/year/year, trend in annual pan evaporation.
Columns 1.12-1.19 refer to secular trends in modeled outputs under the two parameterizations of Ep: columns 1.12-1.15 for the PDSI-based parameterization; columns 1.16-1.19 for the Pan-based parameterization.
1.12 Column "dEp/dt", mm/year/year, trend in annual potential evaporation.
1.13 Column "dETa/dt", mm/year/year, trend in annual evapotranspiration.
1.14 Column "dRO/dt", mm/year/year, trend in annual runoff.
1.15 Column "dSM/dt", mm/year, trend in annual mean soil moisture.
1.16 Column "dEp/dt", mm/year/year, trend in annual potential evaporation.
1.17 Column "dETa/dt", mm/year/year, trend in annual actual evapotranspiration.
1.18 Column "dRO/dt", mm/year/year, trend in annual runoff.
1.19 Column "dSM/dt", mm/year, trend in annual mean soil moisture.

2. **2008gl033840-ts02:** Station climatologies and trends over the periods indicated at the eight New Zealand stations shown in Figure 1 in the text. Population means are derived from the data in this table. Trends are defined as the Ordinary Least Squares-estimated slope of the annual series with respect to time. The residual of the trends in fluxes

(dPrcp/dt - dETa/dt - dRO/dt) equals the second differential of SM with respect to time. Asterisks indicate trends significant at 95%.
Columns 2.1-2.5 refer to station identification and geography.
2.1 Column "NIWA id", the National Institute of Water and Atmospheric Research (NIWA) station identifier.
2.2 Column "Station name, period", the NIWA station name and period for which data are available.
2.3 Column "Long", degrees, station longitude east of Greenwich.
2.4 Column "Lat", degrees, station latitude north of the equator.
2.5 Column "Elev", metres, station elevation above mean sea level.
Columns 2.6-2.11 refer to climatological means and secular trends in observations of model inputs.
2.6 Column "Prcp", mm/year, mean annual precipitation.
2.7 Column "Tair", degrees C, mean annual air temperature.
2.8 Column "Epan", mm/year, mean annual pan evaporation.
2.9 Column "dPrcp/dt", mm/year/year, trend in annual precipitation.
2.10 Column "dTair/dt", degrees C/decade, trend in annual air temperature.
2.11 Column "dEpan/dt", mm/year/year, trend in annual pan evaporation.
Columns 2.12-2.19 refer to secular trends in modeled outputs under the two parameterizations of Ep: columns 2.12-2.15 for the PDSI-based parameterization; columns 2.16-2.19 for the Pan-based parameterization.
2.12 Column "dEp/dt", mm/year/year, trend in annual potential evaporation.
2.13 Column "dETa/dt", mm/year/year, trend in annual evapotranspiration.
2.14 Column "dRO/dt", mm/year/year, trend in annual runoff.
2.15 Column "dSM/dt", mm/year, trend in annual mean soil moisture.
2.16 Column "dEp/dt", mm/year/year, trend in annual potential evaporation.
2.17 Column "dETa/dt", mm/year/year, trend in annual actual evapotranspiration.
2.18 Column "dRO/dt", mm/year/year, trend in annual runoff.
2.19 Column "dSM/dt", mm/year, trend in annual mean soil moisture.

2008gl033840-txts01.pdf

Supporting Information
for
Revisiting the parameterization of potential evaporation as a driver of long-term water balance trends.

Michael T. Hobbins, Aiguo Dai, Michael L. Roderick, and Graham D. Farquhar

This supporting information includes details on the formulation of the E_{pPDSI} parameterization and the sources and infilling of the data used in both E_p parameterizations. Long-term climatological means and estimates of trends of all inputs to, and selected outputs from, the PDSI model at each of the 27 Australian and eight New Zealand stations for both E_p parameterizations are included in tabular form.

SI.1 E_p parameterization details

SI.1.1 Definitions

In the literature of analyses of long-term trends in evaporative measures, it is important to distinguish between the different measures and calculations of evaporation and evapotranspiration.

Thornthwaite [1948] originally defined potential evapotranspiration as the maximum rate of evapotranspiration from a large area covered completely and uniformly by an actively growing vegetation with adequate moisture at all times. However, this concept is not clearly enough specified to function as "an unequivocal parameter" [Brutsaert, 1982], as it confounded the physics of a climatic parameter with a biological component. Thus two further measures evolved: potential evaporation (E_p); and reference crop evapotranspiration (ET_o).

E_p, "Potential evaporation", is defined as the evaporation rate from any large uniform surface sufficiently moist that air in contact with it is saturated. Clearly, this concept does not incorporate a biologic component, so, for instance, the physiological response of plants to water limitations and/or their stomatal response to elevated temperatures are not relevant. Evaporation from a Class-A pan (E_{pan}) defines a potential evaporation rate when it is scaled to account for the additional energy intercepted by the pan-walls. E_{pan} is reliant solely on the same physical drivers of the evaporative process invoked by this concept of potential evaporation, and it similarly disregards biological limitations. In the PDSI bucket model, evaporative demand is a purely physical (i.e., non-biological) parameter: the variation of transpiration is implicitly modeled by the two-layer soil column.

ET_o, "Reference crop evapotranspiration", is a conceptual flux that meters the evaporative demand of the atmosphere as the evapotranspiration that would take place under strictly prescribed biologic and surface moisture conditions: a well-watered grass some 0.12 m high, actively growing and completely shading the ground, with a canopy resistance (r_s) of 70 s/m and an albedo of 0.23 [Allen et al., 1998]. As its biologic component is completely constrained, only climatic factors effect changes in ET_o. ET_o is generally estimated from a specific case of the Penman-Monteith equation, which uses all physical drivers of the evaporative process—net radiation, humidity, temperature, and wind speed—and further allows for a biological limitation on evapotranspiration in the form of resistance parameters related to the stomatal (r_s) and aerodynamic (r_a)

characterisitcs of the canopy. It is widely regarded as the most physically reliable approach to estimate evapotranspiration in many climates when the data are available. ET_o is not relevant to the current study as the biology explictly encoded in its surface parameter (r_s) is implicit in the PDSI bucket model; discussion here is included merely to provide a more complete context.

SI.1.2 Implementation of E_{pPDSI}

The E_{pPDSI} parameterization was proposed by W. C. Palmer and implemented by T. R. Karl (Personal comm., 2007), with the particular formulation used dependent on T_{air}. In freezing conditions, E_{pPDSI} is set to zero (equation (S1)); between 0 °C and 26.67 °C (80 °F), E_{pPDSI} becomes a function of mean monthly T_{air} (ºC), mean monthly solar declination (δ, degrees), station latitude (φ, degrees), and two heat factors, B and H, derived from Dai et al. [1998] (equation (S2)); at 26.67 °C and above, the dependence on B and H drops away in favor of a parameterization that suppresses what would otherwise be a rapid increase in E_p with T_{air} (equation (S3)).

for $T_{air} \leq 0$ ºC (S1)

$$E_p^{PDSI} = 0$$

for 0 ºC $< T_{air} <$ 26.67 ºC (S2)

$$E_p^{PDSI} = 25.4 \frac{\tan^{-1}\left(\sqrt{\frac{1+(\delta\tan\varphi)^2}{\delta\tan\varphi}}\right) + 0.0157}{1.57} * \exp\left(-3.863233 + B\left(1.715598 - \ln H + \ln\left(1.8T_{air}\right)\right)\right)$$

and for $T_{air} \geq$ 26.67 ºC (S3)

$$E_p^{PDSI} = 25.4 \frac{\tan^{-1}\left(\sqrt{\frac{1+(\delta\tan\varphi)^2}{\delta\tan\varphi}}\right) + 0.0157}{1.57} * \left(\sin\left(\frac{T_{air}}{31.833} + 0.3925\right) - 0.76\right)$$

where E_p has units of mm/day. The calculations are done monthly. The temperature response of E_{pPDSI} is shown across the range of heat factors and latitudes of the 35 stations for mid-winter and mid-summer in Figure S2. Note from Figure S2 that E_{pPDSI} falls with increasing T_{air} above 38 ºC. While this may be thought of as mimicking a physiological control on potential evapotranspiration at very high temperatures through stomatal shutdown, in theory such a biologic influence would contravenes the purely physical E_p encoded in the PDSI, and, in practice, mean monthly T_{air} did not exceed this threshold anywhere in Australia or New Zealand during our study period.

SI.2 Data sources and infilling

All Prcp, E_{pan}, and T_{air} data were co-located within the same small enclosure at each meteorological site. Data sources are as follows:

- Prcp data were acquired from the monthly Australian Data Archive for Meteorology maintained by the National Climate Centre at the Bureau of Meteorology (BoM) and from the National Institute of Water and Atmospheric Research (NIWA) in New Zealand.
- Australian E_{pan} data were acquired from the BoM network of standardized (and screened) class-A pans (BoM product code: IDCJDCO5.200506). E_{pan} data for New Zealand were obtained from the New Zealand national network of (unscreened) US Class A pans administered by NIWA. Daily E_{pan} data residing in

these databases were summed (and scaled, if necessary) to valid monthly values if at least 25 daily values were reported in the month.

- Daily T_{air} data were derived from weather stations (BoM product code: IDCJHCO2.200506 for Australia, NIWA for New Zealand) either from multiple observations of T_{air} or as the average of daily maximum and minimum temperatures. Daily T_{air} data were averaged to monthly data if at least 25 daily data were reported in the month. To support climate change research in Australia, the BoM have developed a High Quality Annual Temperature (HQAT) database by, for example, homogenizing the data, quality-ranking the stations, and identifying stations of potential urban influence [Della-Marta et al., 2004]. At each site, for each year, an offest was added to the monthly T_{air} data so that its annual mean agreed with that in the HQAT database.
- The two constant heat factors (B and H) necessary for calculation of E_{pPDSI} were used in Dai et al. [1998; 2004]. They were extracted for the stations' locations from 2.5° x 2.5° global grids (see Figures S1b and S1c).
- Available water capacity (AWC) values necessary to specify the depth of the SM bucket were extracted at the stations' locations from a 2.5° x 2.5° global grid per Webb et al. [1993] (see Figure S1a).

As the soil moisture accounting in the PDSI bucket model does not permit missing input data, these were infilled where necessary, as follows: (i) when two or fewer months' data were missing from a year, these data were scaled from their climatological monthly means according to the proportion of the climatological means exhibited by the rest of the year; or (ii) for all months in any year with more than two months' data missing, climatological monthly means were used. For the 27-station Australian set, these two data-infilling methods were applied to (i) 0.26% of months and (ii) 0.49% of years for T_{air}, and (i) 0.46% of months and (ii) 1.11% of years for E_{pan}. For the set of eight stations in New Zealand, these two data-infilling methods were applied to (i) 0.12% of months and (ii) 0.99% of years for Prcp, (i) 0.45% of months and (ii) 1.97% of years for T_{air}, and (i) 2.67% of months and (ii) 2.96% of years for E_{pan}.

SI.3 Station climatologies

Figure S3 portrays the mean climatologies of the 27 Australian and eight New Zealand stations in the familiar Budyko framework [Budyko, 1974], allowing comparison of the long-term mean annual conditions at each station to the water and energy limits on ET_a. The evaporative index is here defined as mean annual ET_a expressed as a proportion of mean annual E_p, and the wetness index as mean annual Prcp expressed as a proportion of mean annual E_p, with E_p defined in both cases as $k.E_{pan}$. Most Australian stations lie against the water limit, indicating that annual ET_a at these stations is constrained mainly by the water available from Prcp. On the other hand, most New Zealand stations lie toward the energy limit, indicating that, to a far greater degree, annual ET_a at the New Zealand stations is constrained by the available energy, as ample water is available for evaporation. In general, then, ET_a in Australia is predominantly water-limited, while ET_a in New Zealand is predominantly energy-limited.

SI.4 Water balance closure

At all stations the water balance closes, so equation (S4), here showing the water balance across the period 1975-2004, applies:

$$SM_{2004} - SM_{1975} = \sum_{i=1975}^{2004} Prcp_i - \sum_{i=1975}^{2004} ET_{ai} - \sum_{i=1975}^{2004} Runoff_i \,, \qquad \text{(S4)}$$

as do the time-trends in the water balance components (equation (S5)):

$$\frac{dPrcp}{dt} - \frac{dET_a}{dt} - \frac{d\left(Runoff + \Delta SM\right)}{dt} = 0\,. \qquad \text{(S5)}$$

In equation (S5), ΔSM is the year-on-year change in SM (i.e., for year i, $\Delta SM_i = SM_i - SM_{i-1}$), so the third term on the LHS represents the time-trend in the annual combined flux into, and Runoff from, the ground surface. It should be noted, however, that trends reported for SM in Tables S1 and S2 refer to trends in the climatologically more relevant mean annual depth of SM, and so have units of mm/year; they are not time-trends in ΔSM and therefore have different dimensions to those in the reported trends in the fluxes of Prcp, ET_a, and Runoff.

2008gl033840-fs01.tiff

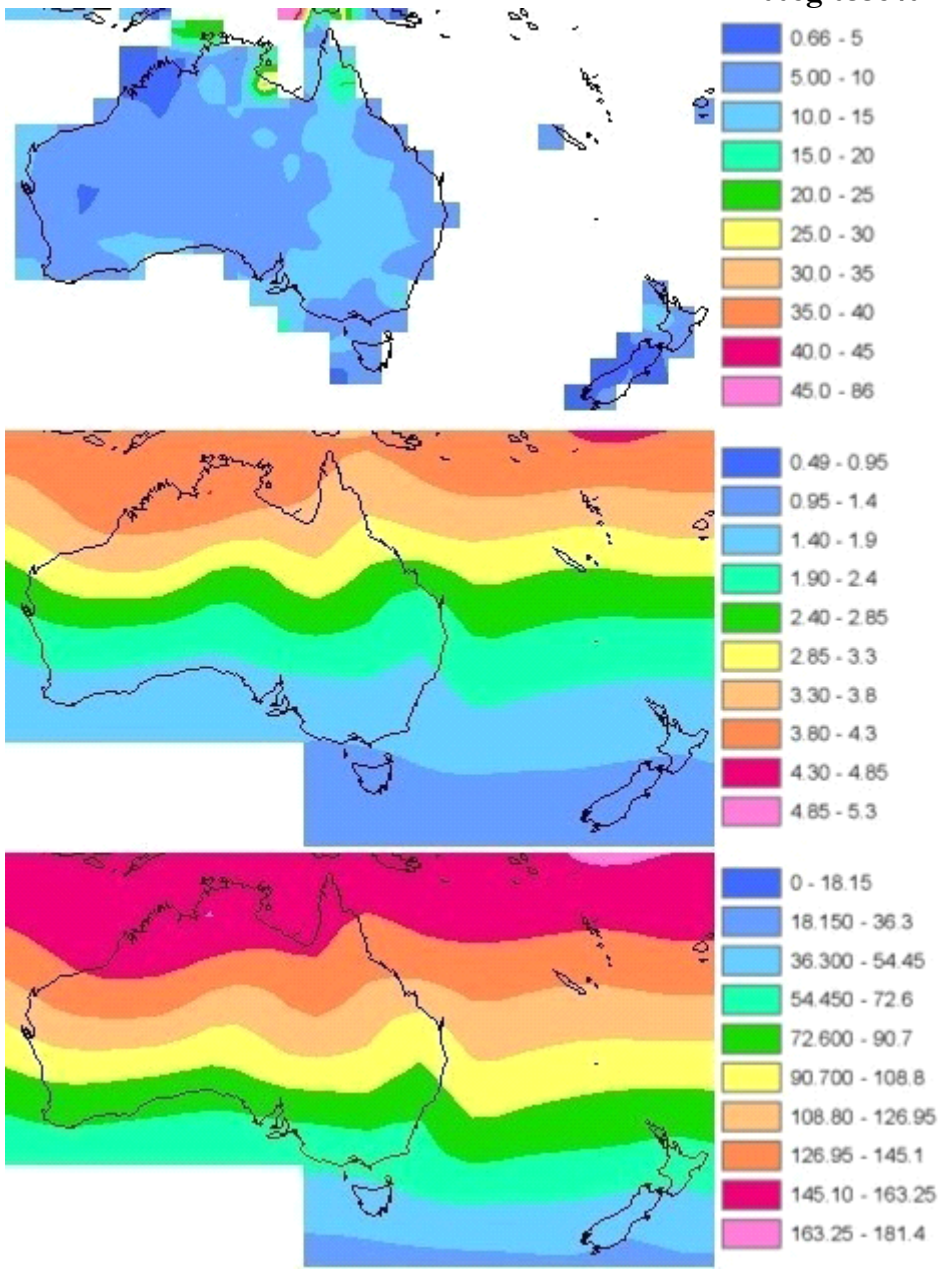

Figure S1: Maps showing distribution across Australia of (a) AWC in inches derived from Webb et al. [1993], (b) heat factor B, and (c) heat factor H. The heat factors are from Dai et al. [1998] and are used to estimate E_{pPDSI} in equation (S2).

2008gl033840-fs02.tiff

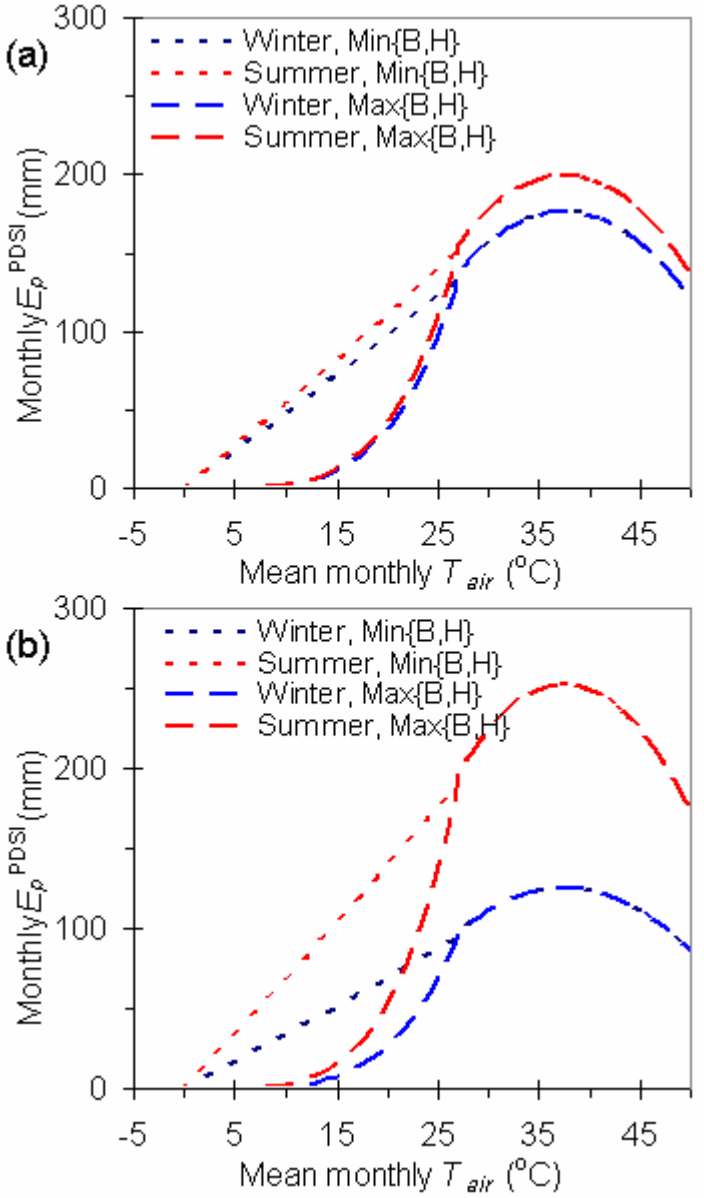

Figure S2: Temperature response of the E_{pPDSI} parameterization at latitudes (a) 10° and (b) 50° using values of heat factors B and H (min{B, H} = {1.038, 33.973}, max{B, H} = {4.266, 162.602}) encompassing the range of the Australian and New Zealand station sets for mid-winter (blue lines) and mid-summer (red lines). Ordinates are monthly E_p depths, abscissae are mean monthly T_{air}.

2008gl033840-fs03.tiff

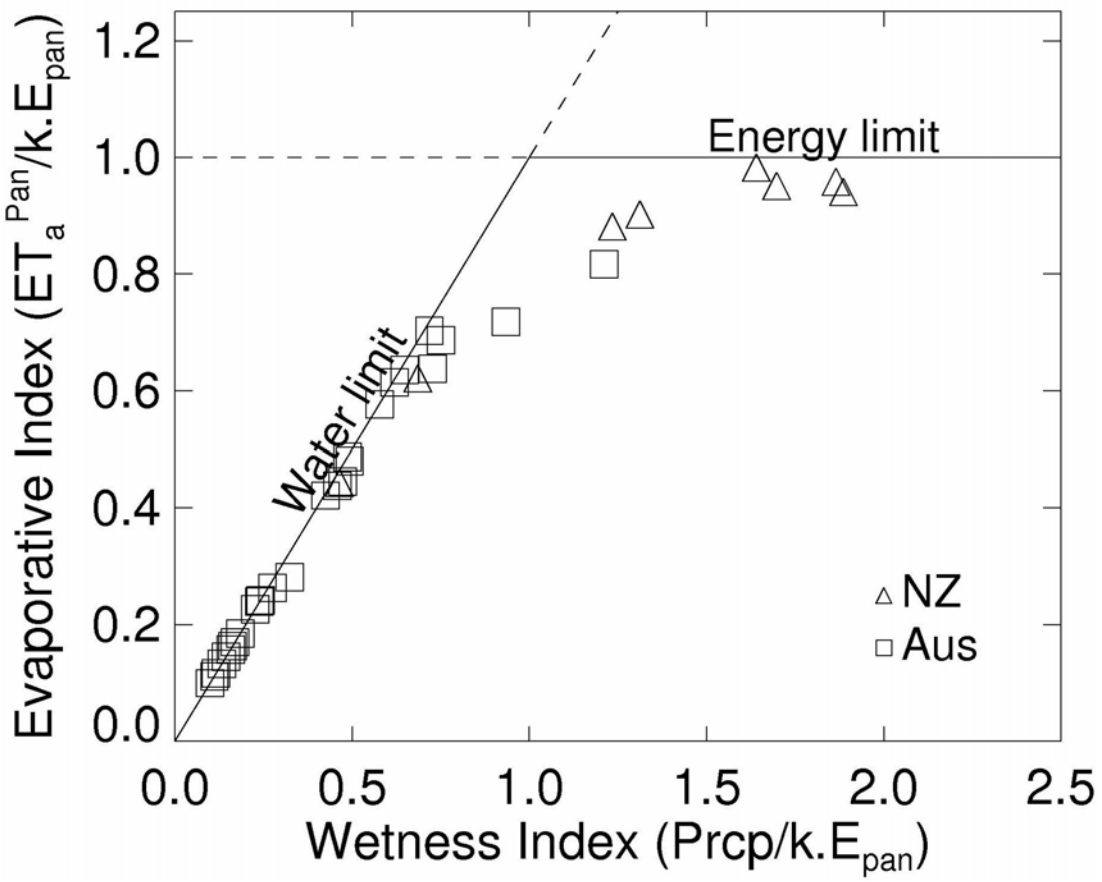

Figure S3: Climatologies of the 27 Australian and eight New Zealand stations within the Budyko framework, as represented by observed Prcp, k.E_{pan}, and modeled ET_{aPan}. Wetness and evaporative indices are derived at each station from their long-term mean annual values. Also indicated are the water- and energy-limits on ET_a.

		Observations						Model output							
		Annual means			Annual trends			PDSI-based annual trends				Pan-based annual trends			
BoM id	Station name Long/Lat/Elev	Prcp	Tair	Epan	δPrcp	δTair	δEpan	δEp	δETa	δRO	δSM	δEp	δETa	δRO	δSM
2012	Halls Creek Airport 127.66/-18.23/422	637	26.9	3093	4.5	0.05	-11.2	0.9	3.3	1.3	0.4	-8.4	3.1	1.4	0.6
3003	Broome Airport 122.23/-17.95/7	665	26.5	2738	6.8	0.13	-9.1*	1.4	6.7	0.1	0.8	-6.8*	6.2	0.7	0.5
4032	Port Hedland Airport 118.63/-20.37/6	320	26.5	3209	1.3	0.20*	7.6	2.2*	1.3	0.0	0.3	5.7	1.3	0.0	0.1
6011	Carnarvon Airport 113.67/-24.89/4	221	22.4	2648	0.6	0.05	-0.5	0.6	0.3	0.0	0.5	-0.4	0.6	0.0	0.3
7045	Meekatharra Airport 118.54/-26.61/517	259	22.5	3475	3.8	-0.03	-17.5*	0.0	3.9	0.0	0.2	-13.1*	3.8	0.0	0.0
8051	Geraldton Airport 114.70/-28.80/33	435	19.9	2429	-0.5	-0.01	-4.4	-0.3	-0.5	-0.2	0.1	-3.3	-0.4	0.0	0.0
9741	Albany Airport 117.80/-34.94/68	792	15.2	1406	-3.0	0.10	5.3*	0.6	0.2	-3.0	-0.5	4.0*	0.8	-3.5*	-1.0*
9789	Esperance 121.89/-33.83/25	603	17.0	1648	1.2	-0.04	1.1	-0.4	1.1	0.5	0.6	0.8	1.4	0.0	-0.1
12038	Kalgoorlie-Boulder Airport 5 121.45/-30.78/36	284	18.6	2614	2.6	0.03	-4.4	-0.3	2.5	0.0	0.2	-3.3	2.6	0.0	0.0
13017	Giles Meteorological Office 128.30/-25.03/598	302	22.7	3472	6.7*	0.06	3.7	0.5	6.7*	0.0	1.0	2.8	6.8*	0.0	0.2
14015	Darwin Airport 130.89/-12.42/30	1805	27.5	2578	4.4	0.24*	-13.8*	2.8*	1.1	1.2	-1.1	-10.4*	-4.2	6.2	1.2
15135	Tennant Creek Airport 134.18/-19.64/376	467	25.9	3965	2.1	0.25	-3.5	3.0	2.1	0.0	0.5	-2.6	2.1	0.0	0.2
18012	Ceduna AMO 133.70/-32.13/15	276	17.0	2248	-0.5	0.09	2.4	0.5	-0.5	0.0	-0.3	1.8	-0.5	0.0	0.0
26021	Mount Gambier Aero 140.77/-37.75/63	705	13.7	1292	2.0	0.13	-6.1*	0.8	0.7	1.2	0.0	-4.5*	0.5	1.4	0.6

30018	Georgetown Post Office 143.55/-18.29/292	780	26.1	2197	-3.7	0.22	-16.6*	2.5	-2.0	-2.1	-0.9	-12.4*	-2.0	-2.1	1.2
31011	Cairns Aero 145.75/-16.87/3	1992	25.0	2194	-8.9	0.19*	7.1*	2.6*	-1.6	-7.5	-3.7*	5.4*	-2.3	-6.7	-3.9*
36031	Longreach Aero 144.28/-23.44/192	420	23.7	3037	-0.1	0.27*	3.6	3.1*	-0.1	0.0	-0.4	2.7	-0.1	0.0	-0.1
39083	Rockhampton Aero 150.48/-23.38/10	741	22.7	2154	-10.3*	0.34*	11.0*	3.8*	-9.4*	-0.7	-1.8	8.2*	-9.7*	-0.5	-0.7
44021	Charleville Aero 146.25/-26.42/302	468	21.0	2584	1.1	0.22	8.7	1.9	1.2	0.0	-0.8	6.5	1.1	0.0	-0.1
48027	Cobar MO 145.83/-31.48/260	403	19.0	2374	-1.1	0.21	-6.9	1.6	-1.2	0.0	-1.0	-5.2	-1.1	0.0	0.0
63005	Bathurst Agricultural Station 149.56/-33.43/713	631	13.3	1360	1.7	0.16	1.0	0.6	2.0*	-0.6	0.4	0.7	1.6	0.3	-0.5
72150	Wagga Wagga AMO 147.46/-35.16/212	569	15.6	1787	-0.6	0.15	-1.9	0.8	0.3	-0.9	-0.1	-1.4	0.0	-0.5	-0.3
76031	Mildura Airport 142.08/-34.23/50	277	16.9	2177	-1.8	0.19*	-8.7*	1.5*	-2.0	0.0	-0.6*	-6.5*	-1.8	0.0	-0.1
82039	Rutherglen Research 146.51/-36.10/175	588	14.5	1591	-2.9	0.05	-5.0	-0.1	-0.8	-2.2	-0.4	-3.8	-2.1	-0.7	-0.2
85072	East Sale Airport 147.13/-38.12/5	581	13.9	1339	-2.1	-0.02	-1.7	-0.3	-1.2	-1.3	-0.1	-1.3	-1.9	-0.6	-0.6
86071	Melbourne Regional Office 144.97/-37.81/31	626	15.8	1162	-1.8	0.15	-10.5*	1.1	-2.2	0.2	-1.3	-7.9*	-2.5	0.8	0.9
91104	Launceston Airport Comparison 147.20/-41.54/170	620	11.8	1273	1.1	-0.09	-1.9	-0.6	0.0	0.5	0.8	-1.5	0.9	-0.2	0.5
------	Population mean	610	20.1	2298	0.1	0.12	-2.7	1.1	0.4	-0.5	-0.3	-2.0	0.2	-0.1	0.0

Table S1: Station climatologies and trends over the period 1975-2004 at the 27 Australian stations shown in Figure 1. Shown are long-term annual mean values for Prcp, Tair and Epan, long-term trends (indicated by δ) in annual Prcp, Tair, and Epan observations and in annual Ep, ETa, Runoff (RO) and SM modeled by both parameterizations. Longitude and latitude are in decimal degrees, elevation in meters above sea level, mean Prcp and mean Epan in mm/year, mean Tair in °C, δPrcp, δEpan, δEp, δETa and δRO in mm/year/year, δTair in °C/decade, and δSM in mm/year. The residual of the trends in fluxes (δPrcp – δETa – δRO) equals the second differential of SM with respect to time. Bold trends are significant at 95%. Population means are derived from the mean of the 27 station-based outputs.

		Observations						Model output							
		Annual means			Annual trends			PDSI-based annual trends				Pan-based annual trends			
NIWA id	Station name, period Long/Lat/Elev	Prcp	Tair	Epan	δPrcp	δTair	δEpan	δEp	δETa	δRO	δSM	δEp	δETa	δRO	δSM
A64282	Leigh 2, 1974-1998 174.80/-36.27/27	1132	15.9	1310	2.7	0.27*	0.9	1.9*	2.5*	0.2	0.1	0.6	2.4	0.5	0.0
B86131	Rotorua Aero 2, 1974-1991 176.32/-38.11/287	1388	12.7	1168	-1.5	0.07	0.4	0.4	0.7	-2.1	0.4*	0.3	2.0*	-3.2	0.9*
C74082	Auckland Aero, 1974-1997 174.79/-37.01/33	1120	15.3	1220	3.0	0.15	-3.6*	1.0	1.9*	1.3	0.1	-2.5*	0.2	3.2	0.2
E14272	Wellington, Kelburn, 1974-2003 174.77/-41.29/125	1250	12.8	947	-12.2*	0.27*	-4.1*	1.6*	0.7	-12.9*	-0.4	-2.8*	-3.5*	-8.8*	-0.2
E15102	Wallaceville, 1977-2002 175.05/-41.14/56	1343	12.4	1028	-8.1*	0.18	-1.3	1.0	1.1	-9.4*	0.0	-0.9	-0.9	-7.5*	0.0
G14711	Grassmere Salt Works, 1974-2003 174.15/-41.73/2	584	13.3	1797	-7.8*	0.40*	-4.7	2.5*	-2.1	-5.2*	-1.6*	-3.3	-5.6*	-2.2	-0.8*
H32451	Christchurch Aero, 1974-1993 172.54/-43.49/37	632	11.4	1317	-6.9*	-0.06	-2.2	-0.5	-1.3	-5.3*	-0.6	-1.5	-2.4	-4.4*	-0.9*
I68433	Invercargill Aero, 1974-2003 168.33/-46.42/0	1116	9.9	972	4.9	0.07	0.4	0.3	0.5	4.8	0.3	0.3	0.6	4.8	0.5
-----	Population mean	1071	13.0	1220	-3.2	0.17	-1.8	1.0	0.5	-3.6	-0.2	-1.2	-0.9	-2.2	0.0

Table S2: Station climatologies and trends over the periods indicated at the eight New Zealand stations shown in Figure 1. Shown are long-term annual mean values for Prcp, Tair and Epan, long-term trends (indicated by δ) in annual Prcp, Tair, and Epan observations and in annual Ep, ETa, Runoff (RO), and SM modeled by both parameterizations. Longitude and latitude are in decimal degrees, elevation in meters above sea level, mean Prcp and mean Epan in mm/year, mean Tair in °C, δPrcp, δEpan, δEp, δETa and δRO in mm/year/year, δTair in °C/decade, and δSM in mm/year. The residual of the trends in fluxes (δPrcp – δETa – δRO) equals the second differential of SM with respect to time. Bold trends are significant at 95%. Population means are derived from the mean of the eight station-based outputs.

References

Allen, R. G., L. S. Pereira, D. Raes, and M. Smith (1998), Crop evapotranspiration - Guidelines for computing crop water requirements - FAO Irrigation and Drainage Paper 56, FAO, Rome.

Brutsaert, W. (1982), Evaporation into the atmosphere: Theory, history and applications, D. Reidel Publishing Company, Dordrecht, Holland.

Budyko, M. I. (1974), Climate and life, Academic Press, New York.

Dai, A., K. E. Trenberth, and T. R. Karl (1998), Global variations in droughts and wet spells: 1900–1995, Geophysical Research Letters, 25 (17), 3367-3370.

Dai, A., T. Trenberth, and K. E. Qian (2004), A global dataset of Palmer Drought Severity Index for 1870-2002: relationship with soil moisture and effects of surface warming, Journal of Hydrometeorology, 5 (December), 117-130.

Della-Marta, P., D. Collins, and K. Braganza (2004), Updating Australia's high-quality annual temperature dataset, Australian Meteorological Magazine, 53, 75-93.

Thornthwaite, C. W. (1948), An approach toward a rational classification of climate, Geographical Review, 38 (1), 55-94.

Webb, R. S., C. E. Rosenzweig, and E. R. Levine (1993), Specifying land surface characteristics in general circulation models: Soil profile data set and derived water-holding capacities, Global Biogeochemical Cycles, 7, 97-108.